The Journal of Infectious Diseases
MAJOR ARTICLE

Zoster-Associated Prothrombotic Plasma Exosomes and Increased Stroke Risk

Andrew N. Bubak,[1] Christina Coughlan,[1] Janelle Posey,[2] Anthony J. Saviola,[3] Christy S. Niemeyer,[1] Serena W.R. Lewis,[1] Sara Bustos Lopez,[1] Adriana Solano,[1] Stephen K. Tyring,[4] Cassidy Delaney,[2] Keith B. Neeves,[2,5] Ravi Mahalingam,[1] Kirk C. Hansen,[3] and Maria A. Nagel[1,6]

[1]Department of Neurology, University of Colorado Anschutz Medical Campus, Aurora, Colorado, USA; [2]Department of Pediatrics, University of Colorado Anschutz Medical Campus, Aurora, Colorado, USA; [3]Department of Biochemistry and Molecular Genetics, University of Colorado Anschutz Medical Campus, Aurora, Colorado, USA; [4]Center for Clinical Studies and Department of Dermatology, McGovern School of Medicine, University of Texas Health Science Center, Houston, Texas, USA; [5]Department of Bioengineering, University of Colorado Anschutz Medical Campus, Aurora, Colorado, USA; and [6]Department of Ophthalmology, University of Colorado Anschutz Medical Campus, Aurora, Colorado, USA

Herpes zoster (HZ; shingles) caused by varicella zoster virus reactivation increases stroke risk for up to 1 year after HZ. The underlying mechanisms are unclear, however, the development of stroke distant from the site of zoster (eg, thoracic, lumbar, sacral) that can occur months after resolution of rash points to a long-lasting, virus-induced soluble factor (or factors) that can trigger thrombosis and/or vasculitis. Herein, we investigated the content and contributions of circulating plasma exosomes from HZ and non-HZ patient samples. Compared with non-HZ exosomes, HZ exosomes (1) contained proteins conferring a prothrombotic state to recipient cells and (2) activated platelets leading to the formation of platelet-leukocyte aggregates. Exosomes 3 months after HZ yielded similar results and also triggered cerebrovascular cells to secrete the proinflammatory cytokines, interleukin 6 and 8. These results can potentially change clinical practice through addition of antiplatelet agents for HZ and initiatives to increase HZ vaccine uptake to decrease stroke risk.

Keywords. varicella zoster virus; exosomes; inflammation; platelet activation; stroke; thrombosis.

Several viruses, including severe acute respiratory syndrome coronavirus 2 (SARS-CoV-2), are associated with stroke, yet mechanisms by which infection triggers disease, even weeks to months after infection has seemingly resolved, are not well characterized. Among these pathogens, stroke associated with varicella zoster virus (VZV) is the most reported. VZV is a double-stranded DNA virus that causes varicella (chickenpox) and then establishes lifelong latency in ganglionic neurons in >95% of Americans [1, 2]. VZV reactivation from ganglia and spread to the corresponding dermatome(s) produces herpes zoster (HZ; shingles), which affects 1 in 3 individuals during their lifetime [3]. HZ is now recognized as a stroke risk factor. In data pooled from 9 studies, stroke relative risk (RR) is 1.78 (95% confidence interval, 1.70–1.88) for the first month following HZ, dropping progressively to 1.20 (1.14–1.26) after 1 year [4]. Stroke risk is higher if HZ is in the ophthalmic distribution (1-month RR, 2.05 [95% confidence interval, 1.82–2.31]) and if HZ occurs in individuals <40 years of age who do not qualify for the HZ vaccine [1-year RR, 2.96 [1.05–8.41]) [4].

The biological basis for HZ-associated stroke has been explained, in part, by direct VZV infection of cerebral arteries leading to vascular inflammation, loss of medial smooth muscle cells, intimal myofibroblast accumulation, and ultimately ischemic or hemorrhagic stroke [5]. Multiple reports point to another, non–mutually exclusive mechanism with VZV infection leading to coagulation abnormalities and development of cerebral venous sinus thrombosis and other thrombotic complications [6–13]. A notable mechanistic feature is the involvement of soluble factors that promote vasculitis or thrombosis distal from the site of rash.

Circulating exosomes have emerged as important "soluble factors" that can affect cells remote from their site of origin. Exosomes are small extracellular vesicles (about 40–160 nm in diameter) of endosomal origin that carry cargo (proteins, nucleic acids) from their cells of origin to adjacent or distal cells for communication during normal and pathological states, regulating biological processes and response to disease [14]. Because previous studies have shown that cancer-derived exosomes can induce platelet activation and aggregation [15, 16], we conducted a pilot study to determine whether plasma exosomes from individuals with HZ, compared with those without HZ, contained factors that would promote platelet activation and thrombosis, potentiating stroke.

METHODS

Standard Protocol Approvals, Registrations, and Patient Consents

Deidentified blood from individuals with HZ was provided by the Center for Clinical Studies in Houston, Texas (collection

Received 12 July 2022; editorial decision 28 September 2022; accepted 04 October 2022; published online 6 October 2022

Correspondence: Andrew N. Bubak, Department of Neurology, University of Colorado School of Medicine, Anschutz Medical Campus, 12700 E 19th Ave, Mail Stop B182, Aurora, CO 80045 (andrew.bubak@cuanschutz.edu).

The Journal of Infectious Diseases® 2023;227:993–1001

https://doi.org/10.1093/infdis/jiac405

protocol approval through the University of Texas Health Science Center's Institutional Review Board; no. HSC-MS-14-0520). Deidentified, non-HZ control blood was obtained commercially from Vitalant.

Non-HZ and HZ Whole-Blood Collection and Plasma Isolation

After informed consent, blood was collected from individuals presenting to the clinic with clinically diagnosed HZ; in addition, samples were collected from 3 of them 2 weeks and 3 months after HZ. Samples were deidentified and sent to University of Colorado–Anschutz Medical Campus (UC-AMC) for plasma isolation and analysis. The HZ group consisted of 13 individuals (5 men, 8 women; mean age, 62.1 years [standard error of the mean, 4.43 years; range, 30–87 years] (Supplementary Table 1); acute HZ samples had previously been analyzed for amyloidogenic peptides and amyloid [17]. For HZ samples, blood was collected within 1 week after rash onset when those with HZ still exhibited a unilateral rash with a dermatomal distribution (Supplementary Table 1); none of the study participants were receiving antiviral therapy at the time of blood collection.

The non-HZ control group included of 10 individuals (5 men, 5 women; mean age, 49.9 years [SEM, 3.33 years; range, 40–67 years] (Supplementary Table 1). Because non-HZ samples were deidentified, additional clinical data were limited, including history of HZ, HZ vaccination, diabetes, or inflammatory disease; however, at the time of blood collection, controls did not exhibit rash and were not acutely ill. Furthermore, per blood donation protocols, control samples were tested and negative on antibody assays for human immunodeficiency virus, hepatitis B and C viruses, and cytomegalovirus. Of note, patients with HZ are not routinely tested for these viruses as part of their standard of care when seen in the clinic; however, the clinical descriptions and medical histories of individuals with HZ herein did not note positivity for any of these viruses.

Exosome Isolation and Validation

Plasma exosomes were isolated using the SmartSEC EV Isolation System (System Biosciences) and then characterized using the NanoSight NS300 instrument (Malvern Panalytical) for size distributions and prepped for mass spectrometry (MS) and platelet activation assays.

MS and Proteomics

Exosome pellets were analyzed by liquid chromatography with tandem MS (LC-MS/MS) by the MS Proteomics Shared Resource Facility located at UC-AMC. Pellets were solubilized in 8 mol/L urea/0.1 mol/L Tris (pH 8.5) and protein concentrations determined using the Pierce BCA Protein Assay Kit (Thermo Fisher Scientific). For each sample, 50 µg of protein as reduced with 5 mmol/L tris(2-carboxyethyl)phosphine for 20 minutes and alkylated with 50 mmol/L 2-chloro-2-iodacetamide for 15 minutes (in the dark and at room temperature [RT]). Samples were diluted with 4 volumes of 100 mmol/L Tris-hydrochloride (pH 8.5) and then digested with sequencing grade trypsin (Promega) at an enzyme-substrate ratio of 1:50 overnight at 37°C. Formic acid (FA) was added to samples to a 5% concentration and tryptic peptides were purified with Pierce C18 tips (Thermo Fisher Scientific) per manufacturer's protocol. Digests were vacuum dried and resuspended in 0.1% FA. LC-MS/MS was performed using an Easy nLC 1200 instrument coupled to a Q-Exactive HF mass spectrometer (Thermo Fisher Scientific). Tryptic peptides were loaded on a C18 column (20 cm with a 100-µm inner diameter) packed in house with a 2.7-µm Cortecs C18 resin column and separated at a flow rate of 0.4 µL/min with solutions A (0.1% FA) and solution B (0.1% FA in ACN) and under the following conditions: isocratic with 4% solution B for 3 minutes, followed by 4%–32% solution B for 102 minutes, 32%–55% solution B for 5 minutes, 55%–95% solution B for 1 minute, and isocratic at 95% solution B for 9 minutes.

LC-MS/MS was performed using a data-dependent acquisition top-15 method with dynamic exclusion set to 20 seconds. Fragmentation spectra were interpreted using the MSFragger-based FragPipe computational platform [18] with the combined UniProtKB/SwissProt human and VZV proteome databases. Reverse decoys and contaminants were included automatically. The precursor mass tolerance and fragment mass tolerance were set to 10 ppm and 0.2 Da, respectively. Cysteine carbamidomethylation was selected as a fixed modification and oxidation as a variable modification. Two missed tryptic cleavages were allowed, and the protein-level false discovery rate was ≤1%. Protein fold changes were calculated by comparing the HZ spectral intensity values of each protein to non-HZ levels. Significant differential expression of identified proteins between HZ and non-HZ samples was determined using the 2-stage step-up method (Benjamini, Krieger, and Yekutieli) with a false discovery rate set at $q < 0.05$ and GraphPad Prism 9 (GraphPad) statistical software. Bioinformatic and enrichment analyses were conducted using the STRING v11 (http://string-db.org) and PANTHER v17 (http://pantherdb.org) databases, which implement well-known classification systems such as Gene Ontology and Kyoto Encyclopedia of Genes and Genomes (KEGG). Figures were produced using GraphPad Prism and BioRender software.

Preparation of Washed Platelet Suspension and Whole Blood for Flow Cytometric Analysis

Study participants were recruited at UC-AMC. Protocol approval was obtained from the Colorado Multiple Institutional Review Board in accordance with the Declaration of Helsinki

(no. 19-2408). It was confirmed that healthy male and female donors had not taken antiplatelet or anticoagulant drugs, acetaminophen, or any nonsteroidal anti-inflammatory drugs for the prior 2 weeks, had consumed no alcohol during the prior 48 hours, and were not pregnant at the time of blood donation.

Washed Platelets

Blood was collected by venipuncture, using a 19-gauge needle into acid-citrate-dextrose (ACD) vacutainer tubes. The first 4.5 mL of blood were discarded. The ACD-anticoagulated whole blood was centrifuged at 100*g* for 20 minutes at RT. Platelet-rich plasma was collected, transferred to a new tube, and supplemented with PGI2 (1 μg/mL; Cayman Chemical) and Apyrase (0.02 U/mL; Sigma-Aldrich) and incubated for 3 minutes at RT. Platelet-rich plasma samples were centrifuged at 2000*g* for 5 minutes, the supernatant was discarded, and the platelet pellet was resuspended in 1 mL of warm Tyrode's buffer, pH 7.3 (sodium chloride, 129 mmol/L; potassium chloride, 2.9 mmol/L; magnesium chloride, 1 mmol/L; monosodium phosphate, 0.34 mmol/L; sodium bicarbonate, 12 mmol/L; and glucose, 5 mmol/L).

Whole Blood

Blood was collected into ACD vacutainer tubes and immediately diluted 1:10 in M199 medium containing 100 U/mL heparin.

Flow Cytometric Assessment of Platelet Activation

Flow cytometry was performed by diluting washed platelets (platelet count, 1×10^6/mL) in 100 μL of warm Tyrode's buffer containing 1 mmol/L calcium chloride. Platelets were activated for 20 minutes at 37°C in the dark with thrombin (0.1 U/mL; Chrono-log), calcimycin (A23187; 5 μmol/L, Sigma-Aldrich), non-HZ or HZ exosomes at 20% per volume in the presence of anti-human CD41-BV421 antibody (Biolegend; clone no. HIP8; 1:20), anti-mouse/human P-selectin–allophycocyanin (Biolegend; clone no. APM-1; 1:25) and anti-mouse/human β-lactadherin–fluorescein isothiocyanate FITC (Prolytics, 1:20). Unstained and fluorescence-minus-one controls were used to determine monoclonal antibody (mAb) gating.

Two platelet agonists, thrombin and calcimycin, were used as controls as they activate platelets via different mechanisms, leading to unique subpopulations of activated platelets. Thrombin activates human platelets via protease-activated receptors 1 and 4 [19], leading to release of α-granule proteins, including P-selectin. Calcimycin causes non–receptor-mediated activation of platelets via elevation of intracellular calcium ion concentration, which induces the translocation of phosphatidylserine (PS) to the platelet surface, producing procoagulant platelet subpopulations [20, 21]. The assay was quenched at 20 minutes by diluting blood 1:5 with RT 1% paraformaldehyde (PFA) in Tyrode's buffer. Platelets were differentiated from white blood cells and debris by size using forward and side scatter and were defined as $CD41^+$. For P-selectin and PS detection in platelets, 100 000 platelets were captured and analyzed for expression of P-selectin and β-lactadherin (PS). Samples were run on the Gallios 561 analyzer (Beckman Coulter). Specific mAb binding was expressed as the percentage of positive cells. Flow cytometry data were analyzed using Kaluza flow analysis software (Beckman Coulter).

Flow Cytometric Assessment of Platelet-Leukocyte Aggregates

For characterization of platelet-leukocyte aggregates, 200 μL of diluted, citrated blood was aliquoted into 2.0-mL tubes. Non-HZ or HZ exosomes were added at 20% per volume in the presence of anti-human CD41-BV421 antibody (Biolegend; clone no. HIP8; 1:20), anti-human CD45 (BD Biosciences; clone no. 2D1; 1:20), anti-human CD15-phycoerythrin/cyanine 7 (Biolegend; clone no. W6D3; 1:20), and anti-human CD14-phycoerythrin (Biolegend; clone no. 63D3; 1:20). Blood samples were stained for 20 minutes at 37°C in the dark. The assay was quenched using 1.5 mL of BD fluorescence-activated cell sorting lysis buffer and fixed for 15 minutes. Samples were centrifuged at 800*g* for 5 minutes, supernatant was discarded, and fixed cells were resuspended in BD fluorescence-activated cell sorting lysis buffer. To classify platelet-leukocyte aggregates, 20 000 leukocytes were captured and segregated using basic side-scatter property discrimination (side-scatter area × forward scatter) and $CD45^+$. Leukocyte subtype-specific antibodies were used to confirm leukocyte populations: neutrophils ($CD14^{+lo}$, $CD15^+$) and monocytes ($CD14^{+hi}$, $CD15^-$). Total leukocytes, monocytes, and neutrophils were analyzed for CD41 positivity to measure the percentage of platelet-leukocyte, platelet-monocyte, and platelet-neutrophil aggregates. Specific mAb binding was expressed as the percentage of positive cells in the target gate. Samples were run on the Gallios 561 analyzer (Beckman Coulter). Data were analyzed using Kaluza flow analysis software (Beckman Coulter; example of gating strategy shown in Supplementary Figures 2 and 4).

Vascular Cell Culturing and Proinflammatory Enzyme-Linked Immunosorbent Assays

Quiescent primary human brain vascular adventitial fibroblasts were prepared in 12-well plates, as described elsewhere [22]. Cells were exposed to vehicle (phosphate-buffered saline), non-HZ exosomes, or exosomes 3 months after HZ (20% total volume of culture medium) and supernatant collected 36 hours later. Owing to limited sample availability, samples from 2 weeks after HZ were not analyzed. Supernatant samples were assayed in duplicate for interleukin 6 and 8 (IL-6 and IL-8; Abcam; catalog nos. ab178013 and ab214030, respectively) via enzyme-linked immunoassay. To determine the statistical significance of difference between groups, a 1-way analysis of variance with a Tukey correction for multiple comparisons, was used with α set at $P < .05$.

RESULTS

Unique Proteins Associated With Infectious and Immunoregulatory Pathways in HZ Plasma Exosomes

Plasma samples were collected from 13 individuals with acute HZ and 10 without HZ; of the 13 with HZ, 3 (HZ8, HZ9, and HZ13) also provided samples 2 weeks and 3 months after HZ. Exosomes were extracted, and a subset analyzed by means of (1) nanoparticle tracking analysis with mean and mode particle sizes of 139.4 (standard error of the mean, 14.27) nm and 86.9 (49) nm, respectively (Figure 1*A*), consistent with exosome size range [14], and (2) MS, detecting 590 total unique molecules—all of human origin. Of these proteins, 86 were significantly up-regulated in HZ exosomes compared with non-HZ exosomes; there were no significantly down-regulated proteins (Supplementary Table 2). Non-HZ and HZ exosomes did not contain VZV proteins and were noninfectious; a subset (HZ8, HZ9, and HZ13) applied to uninfected cells produced no cytopathic effect (data not shown). Principal component analysis revealed clear clustering of samples between non-HZ and HZ groups (Figure 1*B*); no distinct clustering was observed when HZ samples were independently analyzed by rash location (HZ ophthalmicus vs cervical, thoracic, lumbar, and sacral HZ; Figure 1*C*). Enrichment analyses of all identified molecules revealed protein lists consistent with extracellular exosomes, blood microparticles, and vesicles, confirming that the isolated plasma particles were of predominantly exosomal origin (Figure 1*D*).

HZ exosomes contained 41 molecules that were not detected in non-HZ exosomes (Figure 1*E* and Supplementary Table 3), of which 18 molecules were in a vast majority of HZ samples (10–13 of 13 total HZ samples), and the remaining 23 molecules were in 7–9 of 13 total HZ samples. The functions of these molecules were predominantly associated with protein, ion, and carbohydrate derivative binding, as well as hydrolase, oxidoreductase, and ligase activity (Figure 1*E*). Overall, compared with non-HZ exosomes, HZ exosomes contained 127 notable proteins, of which 86 were significantly up-regulated and 41 were found only in HZ exosomes (Figure 2*A* and Supplementary Tables 2 and 3, respectively). The up-regulated molecules had a significant interaction enrichment (adjusted $P < .001$) among themselves, more than would be expected for a random set of

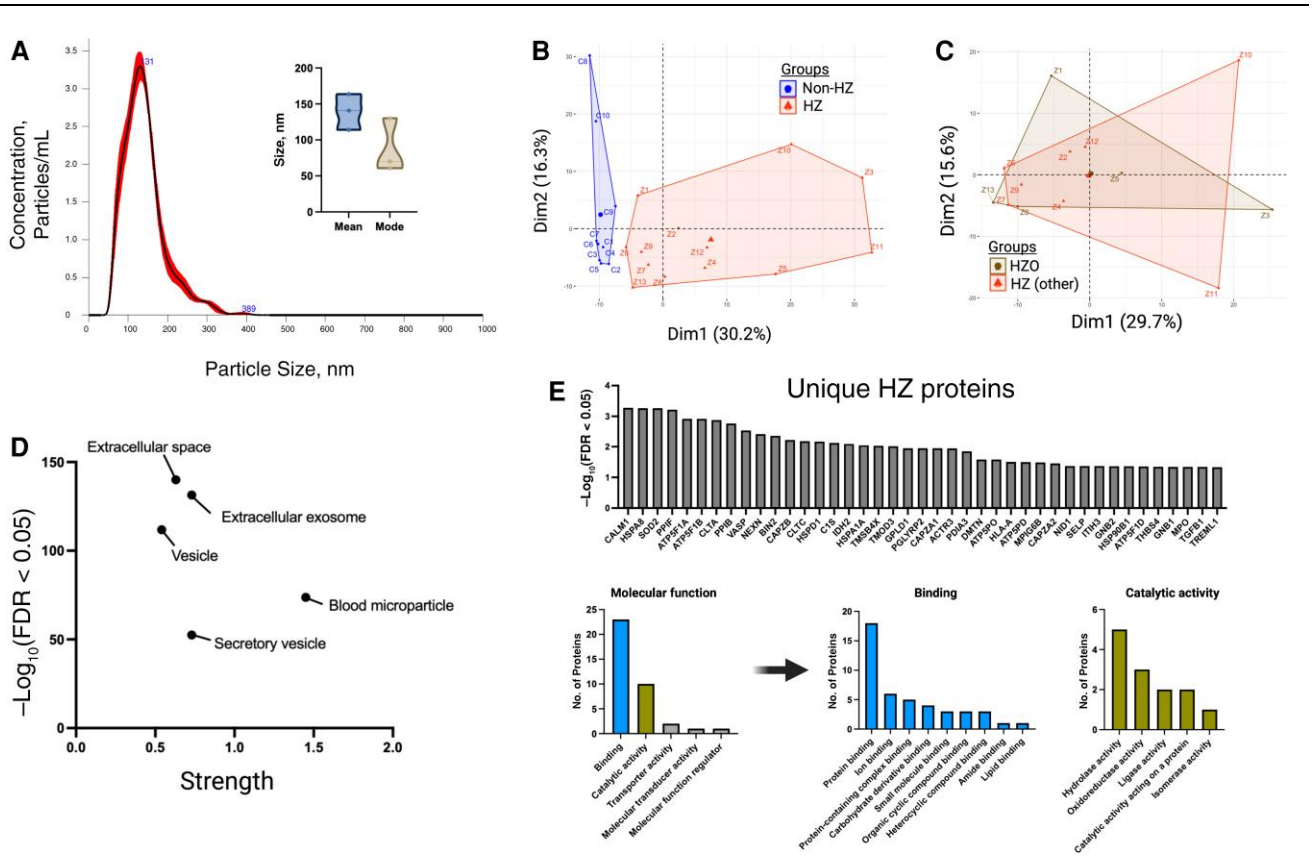

Figure 1. Proteomic analysis of herpes zoster (HZ) and non-HZ plasma exosomes. *A,* Nanoparticle tracking analysis of a subset of non-HZ plasma exosomes (n = 3) revealing size distribution (histogram) and the mean and mode (inset). *B,* Principal component analysis of non-HZ versus acute HZ exosome content. Abbreviations: Dim1, Dimension 1; Dim2, Dimension 2. *C,* Principal component analysis within the HZ group, separated by rash location (HZ ophthalmicus [HZO] or HZ in any other distribution). *D,* Protein enrichment analysis of total exosome content across groups. Abbreviation: FDR, false discovery rate. *E,* Unique proteins in HZ samples and the breakdown of molecular function. Abbreviations of proteins used approved HUGO Gene Nomenclature Committee (HGNC) format (https://www.genenames.org).

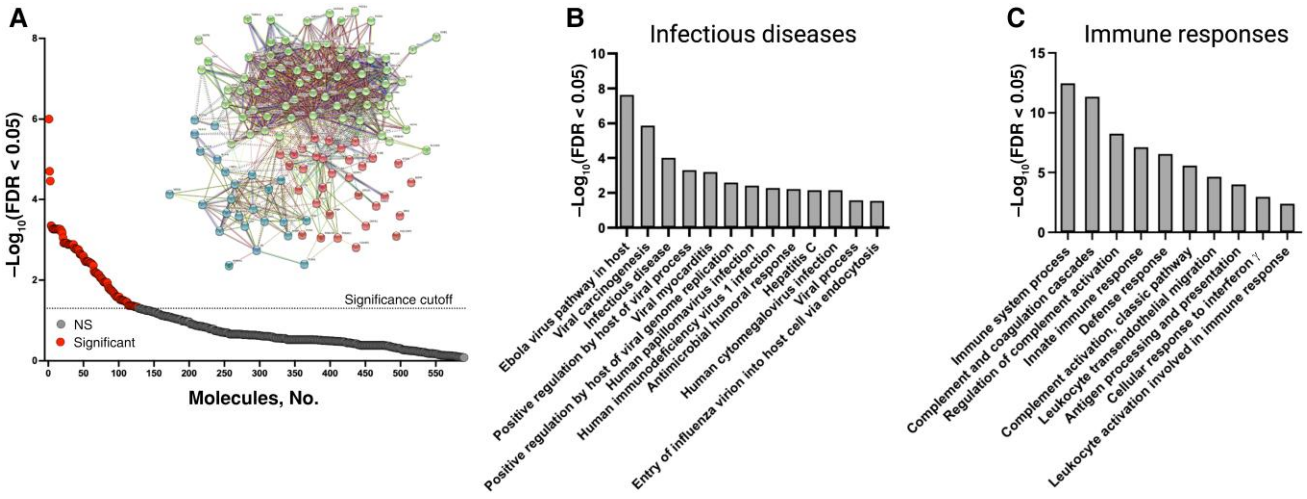

Figure 2. Herpes zoster (HZ) exosomes were enriched for pathways associated with infectious diseases and immune responses. *A,* Proteins significantly elevated in HZ exosomes (*above dotted line*; n = 127) compared with non-HZ exosomes, along with the interaction network of these proteins (*inset*). Abbreviations: FDR, false discovery rate; NS, not significant. *B, C,* Protein enrichment analyses associated with infectious diseases (*B*) and immune responses (*C*).

molecules of the same size and degree of distribution drawn from the genome, indicating that the significantly elevated molecules are biologically connected (Figure 2*A* inset; k-means clustering set to 3 groups). Pathway enrichment analyses of the significantly elevated molecules in HZ exosomes revealed pathways involved in infectious diseases, including positive regulation by the host of the viral process/genome replication, viral carcinogenesis, and viral myocarditis (Figure 2*B* and Supplementary Table 4). Similarly, significant enrichment of immune response pathways was detected, including complement activation, leukocyte transendothelial migration, cellular response to interferon γ, and antigen processing and presentation (Figure 2*C* and Supplementary Table 4).

Enrichment of Cerebrovascular and Cardiovascular Disease Pathways in HZ Exosomes

Further enrichment analyses of HZ compared with non-HZ exosomes revealed pathways associated with platelet activation, signaling and aggregation, blood coagulation, hypertrophic cardiomyopathy, and fibrin clot formation (Figure 3*A* and Supplementary Table 4). Specific proteins significantly elevated in HZ exosomes and involved in platelet activation, signaling, and aggregation included thrombospondin 1, caveolae-associated protein 2, coagulation factor V, and coagulation factor XIII A1 chain (Figure 3*B*). Cardiovascular system disease proteins elevated in HZ exosomes included calmodulin 1 and transthyretin (Figure 3*C*). Transthyretin is also involved in cardiac amyloidosis [23], which is intriguing given previous studies demonstrating that plasma from patients with acute HZ contains elevated amyloid and is amyloidogenic [17]. Stroke can occur months after HZ [24]; therefore, we tested a subset of exosomes that were available 2 weeks and 3 months after HZ. The proteins of interest elevated at the acute time point remained elevated up to 3 months after HZ (Supplementary Figure 1).

Prothrombotic and Proinflammatory Activity in HZ Plasma Exosomes

To determine the functional significance of these exosomes in the context of HZ-associated vascular disease, we exposed human platelets to HZ or non-HZ exosomes and then measured P-selectin and PS expression; these markers are up-regulated in platelets following activation, supporting platelet-endothelial and/or platelet-leukocyte adhesion and thrombin generation, respectively [20, 21, 25]. Compared with non-HZ exosomes, HZ exosome-exposed platelets had a significantly higher expression of both P-selectin and PS; this effect remained in the 3-month post-HZ exosome samples (Figure 4*A*, *upper panels,* and Supplementary Figures 2 and 3). Of note, P-selectin was detected at higher levels in HZ exosome samples than in non-HZ samples, suggesting that the elevation in platelet P-selectin may be partially due to HZ exosome-delivered cargo; however, PS was not detected in any exosome samples, indicating that HZ exosomes induced its expression in platelets.

To corroborate these functional findings, we exposed platelets to HZ or non-HZ exosomes and found that exposure to HZ exosomes, but not non-HZ exosomes, resulted in a significant increase in leukocyte (monocyte and neutrophil) aggregates (Figure 4*A*, *lower panels,*and Supplementary Figure 4); exosomes from 3-month post-HZ samples were not significantly different from non-HZ exosomes (Figure 4*A*, *lower panels*). Finally, given that persistent inflammation is a hallmark of HZ and HZ-associated diseases, we tested whether these later time points can induce a proinflammatory

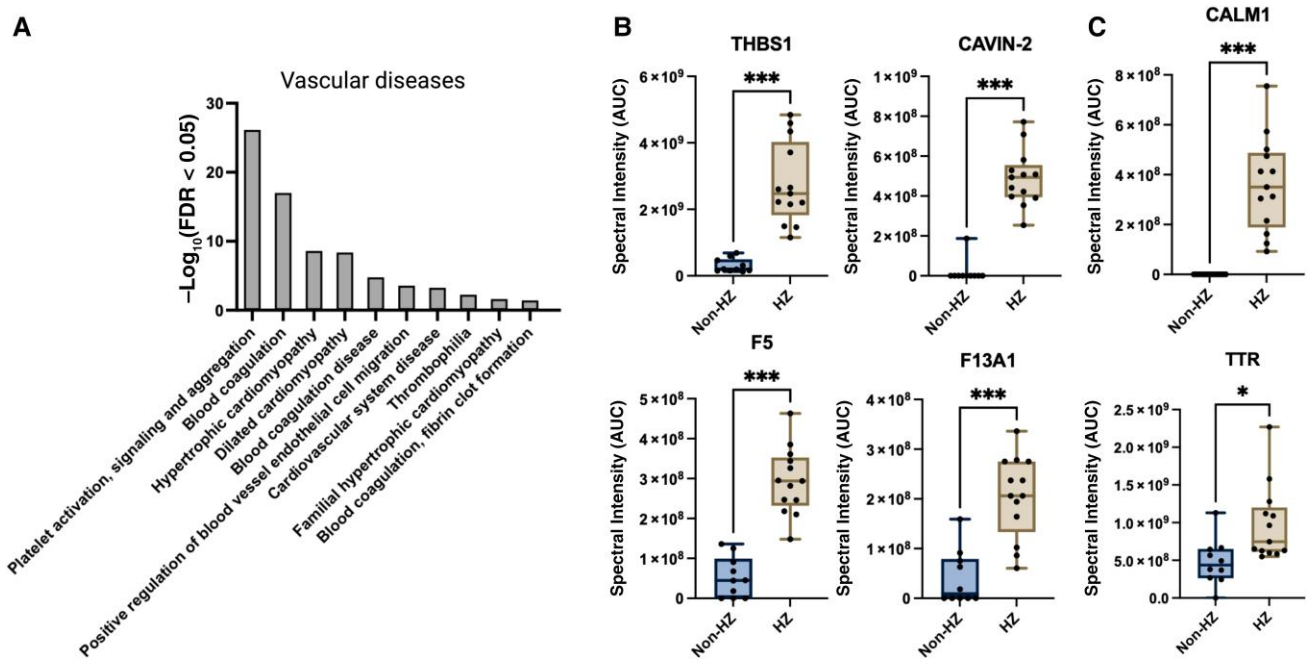

Figure 3. Identification of herpes zoster (HZ) exosomal proteins involved in vascular disease. *A,* Proteins from HZ exosomes were significantly enriched for pathways associated with vascular disease. Abbreviation: FDR, false discovery rate. *B, C,* Specific proteins associated with platelet activation, signaling, and aggregation pathways (*B*) as well as cardiovascular system disease pathways (*C*), compared between HZ and non-HZ exosomes. Individual samples are shown as dots on the graph; box plots show minimum and maximum values (error bars) and means. Abbreviations: AUC, area under the curve; CALM1, calmodulin 1; CAVIN-2, caveolae associated protein 2; F5, coagulation factor V; F13A1, coagulation factor XIII A1 chain; THBS1, thrombospondin; TTR, transthyretin. **P* = .03; ****P* < .001.

environment by exposing naive human brain vascular adventitial fibroblasts to non-HZ and 3-month post-HZ exosomes and then measuring secreted IL-6 and IL-8; these cytokine levels are elevated during VZV infection in vitro and in vivo [26, 27]. Compared with non-HZ exosomes, those from 3-month post-HZ samples significantly increased human brain vascular adventitial fibroblast secretion of IL-6 and IL-8 (Figure 4*B*).

DISCUSSION

In the current study, we found that prothrombotic, proinflammatory plasma exosomes are present during acute HZ and can persist up to 3 months, providing a novel noninfectious mechanism by which VZV, and likely other viruses, increases stroke risk. The origins of the heterogenous population of exosomes remain to be determined, but a subset most likely originates from ganglionic neurons, where latent VZV reactivated and replicated. Given that exosomes are produced continuously, the presence of these pathogenic exosomes 3 months after HZ raises the possibility of ongoing low-grade viral replication in ganglionic neurons, resulting in continued pathogenic exosome production despite clearance of rash.

Support for ongoing viral replication after HZ comes from (1) intermittent shedding of VZV DNA in saliva of some individuals with HZ (67%) up to 12 years after HZ compared with none in non-HZ controls [28]; (2) detection of VZV DNA in peripheral blood mononuclear cells (PBMCs) of individuals with HZ up to 7 weeks later [29]; (3) intermittent VZV DNA in PBMCs that disappeared during bouts of antiviral therapy in an individual with postherpetic neuralgia [30], as well as detection of VZV DNA in the PBMCs of 33% of patients with postherpetic neuralgia in serially obtained blood samples ≥1 year after HZ [31]; and (4) the presence of VZV antigen and DNA in postmortem trigeminal ganglia from an individual with HZ 2 years earlier [32]. These findings suggest that VZV does not return to latency in a subset of individuals and that a prolonged prothrombotic state may continue after completion of antiviral therapy and clearance of rash. With regard to clinical management, our findings suggest a potential role for longer duration antiviral therapy, in addition to antiplatelet and anti-inflammatory agents, as well as initiatives to increase HZ vaccine uptake to decrease stroke risk [33], particularly in individuals with known stroke risk factors, including preexisting atherosclerosis, stenosis, and coagulation deficits.

A limitation of the current study is its small sample size (acute HZ, n = 13; 2 weeks and 3 months after HZ, n = 3). Specifically, our study primarily focused on acute HZ time points with no adverse vascular events seen in the short follow-up period. Although we recorded statistically significant changes during acute HZ and 3 months after HZ with respect to

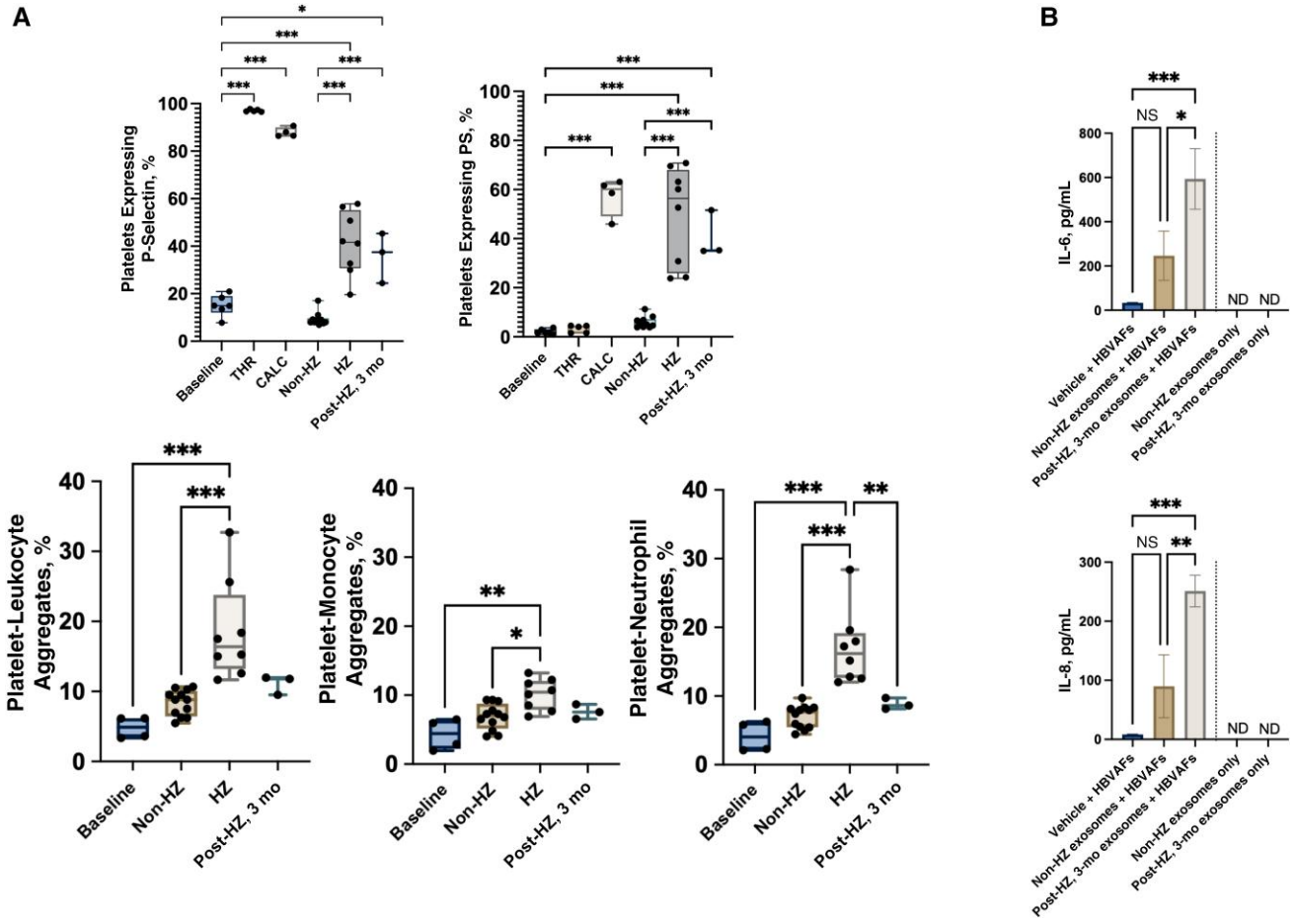

Figure 4. Herpes zoster (HZ) exosomes activate platelets and induce interleukin 6 and 8 (IL-6 and IL-8) secretion. *A, Upper panels,* Acute HZ or 3 month post-HZ exosome treatment increased platelet P-selectin (baseline) (*left*) and phosphatidylserine (PS) (*right*) expression (positive controls; thrombin [THR] and calcimycin [CALC]). Non-HZ exosomes had no effect on platelet activation. Individual samples are shown as dots on graph. *Lower panels,* Acute HZ but not 3-month post-HZ exosomes increased platelet-leukocyte (*left*), platelet-monocyte (*middle*), and platelet-neutrophil (*right*) aggregation. Expression and aggregation were analyzed by means of flow cytometry; box plots show minimum and maximum values (error bars) and means. *B,* Secreted IL-6 (*top*) and IL-8 (*bottom*) levels from primary human brain vascular adventitial fibroblasts (HBVAFs) exposed to vehicle, non-HZ, or 3-month post-HZ exosomes. IL-6 and IL-8 were not detected (ND) in the input non-HZ or HZ exosomes. $^{*}P = .03$; $^{**}P = .002$; $^{***}P < .001$; NS, not significant.

platelet activation and induction of inflammation with this small cohort, follow-up studies extending to 1 year after HZ with a larger cohort are warranted to consider temporal changes in exosome prothrombotic and proinflammatory activity, comorbid conditions (eg, diabetes mellitus, hypertension, hyperlipidemia, and tobacco use), and development of vascular complications. In addition, a wider range of ages will be informative, given that elevated stroke risk following HZ is greater in individuals <40 years of age than in all other age groups [4]. The HZ group in the current study had a higher mean age (62 years); we would hypothesize that the prothrombotic and proinflammatory state conferred by pathogenic exosomes would be even higher in a younger HZ group (aged <40 years), consistent with epidemiological data [4]. Importantly, this younger group is not eligible for the HZ vaccine, further compounding risk. While our study found prothrombotic exosomes in individuals with HZ, it is possible that similar pathogenic exosomes are generated during varicella, leading to thrombotic complications. This is supported by reports of cerebral venous thrombosis and pulmonary embolism associated with varicella [10, 12, 13, 34]. However, a future study using varicella samples is required to support this hypothesis.

Our findings open new avenues of research to explore pathogenic exosomes that increase stroke risk and their persistence in other viral infections. Of particular importance is the role of persistent prothrombotic exosomes in stroke associated with SARS-CoV-2 infection because thrombotic complications have been observed months after coronavirus disease 2019 (COVID-19) or asymptomatic infection [35, 36]. In these cases, SARS-CoV-2 infection may produce pathogenic, prothrombotic exosomes. However, it is also possible that VZV reactivation and HZ exosomes are an additional contributor to

COVID-19–associated strokes; a study published in 2022 showed that individuals aged ≥50 years with COVID-19 are 15% more likely to develop HZ, and 21% more likely if hospitalized [37]. Overall, our tantalizing results change the paradigm of infectious disease—once infection has resolved, disease is not over; persistent exosomes may continue to trigger pathological responses thought to be unrelated to and distant from the site of the original infection.

Supplementary Data

Supplementary materials are available at *The Journal of Infectious Diseases* online. Consisting of data provided by the authors to benefit the reader, the posted materials are not copyedited and are the sole responsibility of the authors, so questions or comments should be addressed to the corresponding author.

Notes

Acknowledgments. The authors thank Cathy Allen and Teresa Mescher for manuscript preparation.

Financial support. This work was supported by the National Institutes of Health (grants P01 AG032958 to A. N. B. and M. A. N., P01 HL152961 to C. D., and R33HL141794, R21HL152350, and R01HL151984 to K. B. N.) and the National Cancer Institute (Cancer Center Support Grant P30 CA046934 to the Flow Cytometry Shared Resource and Proteomics Facility at the University of Colorado Comprehensive Cancer Center, which provided cytometry and proteomics services.

Potential conflicts of interest. All authors: No reported conflicts. All authors have submitted the ICMJE Form for Disclosure of Potential Conflicts of Interest. Conflicts that the editors consider relevant to the content of the manuscript have been disclosed.

References

1. Fairley CK, Miller E. Varicella-zoster virus epidemiology—a changing scene? J Infect Dis **1996**; 174:S314–9.
2. Reynolds MA, Kruszon-Moran D, Jumaan A, Schmid DS, McQuillan GM. Varicella seroprevalence in the U.S.: data from the National Health and Nutrition Examination Survey, 1999–2004. Public Health Rep **2010**; 125:860–9.
3. Harpaz R, Ortega-Sanchez IR, Seward JF. Prevention of herpes zoster: recommendations of the Advisory Committee on Immunization Practices (ACIP). MMWR Recomm Rep **2008**; 57:1–30; quiz CE2-4.
4. Marra F, Ruckenstein J, Richardson K. A meta-analysis of stroke risk following herpes zoster infection. BMC Infect Dis **2017**; 17:198.
5. Nagel MA, Bubak AN. Varicella zoster virus vasculopathy. J Infect Dis **2018**; 218:S107–12.
6. Fluri S, Kaczala GW, Leibundgut K, Alberio L. Chickenpox is not always benign: postvaricella purpura fulminans requires prompt and aggressive treatment. Pediatr Emerg Care **2010**; 26:932–4.
7. Sharma VK, Dubey TN, Dave L, Agarwal A. Postvaricella purpura fulminans with no evidence of disseminated intravascular coagulation (DIC) or protein S deficiency. J Indian Med Assoc **2010**; 108:529–30.
8. Siddiqi SA, Nishat S, Kanwar D, Ali F, Azeemuddin M, Wasay M. Cerebral venous sinus thrombosis: association with primary varicella zoster virus infection. J Stroke Cerebrovasc Dis **2012**; 21:917.e1–4.
9. Maity PK, Chakrabarti N, Mondal M, Patar K, Mukhopadhyay M. Deep vein thrombosis: a rare signature of herpes zoster. J Assoc Physicians India **2014**; 62:72–4.
10. Khan R, Yasmeen A, Pandey AK, Al Saffar K, Narayanan SR. Cerebral venous thrombosis and acute pulmonary embolism following varicella infection. Eur J Case Rep Intern Med **2019**; 6:001171.
11. Zhu R, Fang C, Wang J, He X. Acute herpes zoster followed by cerebral venous sinus thrombosis. Neurol India **2020**; 68:219–21.
12. Badour M, Shhada E, Hammed A, Baqla S. Cerebral venous sinus thrombosis as a complication of primary varicella infection in a child, case report. Ann Med Surg (Lond) **2021**; 73:103165.
13. Alamlih L, Abdulgayoom M, Menik Arachchige SN, Shah MH, Zahid M. Chronic headache and cerebral venous sinus thrombosis due to varicella zoster virus infection: a case report and review of the literature. Am J Case Rep **2021**; 22:e927699.
14. Kalluri R, LeBleu VS. The biology, function, and biomedical applications of exosomes. Science **2020**; 367:eaau6977.
15. Gomes FG, Sandim V, Almeida VH, et al. Breast-cancer extracellular vesicles induce platelet activation and aggregation by tissue factor-independent and -dependent mechanisms. Thromb Res **2017**; 159:24–32.
16. Almeida VH, Rondon AMR, Gomes T, Monteiro RQ. Novel aspects of extracellular vesicles as mediators of cancer-associated thrombosis. Cells **2019**; 8:716.
17. Bubak AN, Beseler C, Como CN, et al. Acute zoster plasma contains elevated amyloid, correlating with Aβ42 and amylin levels, and is amyloidogenic. J Neurovirol **2020**; 26: 422–8.
18. Kong AT, Leprevost FV, Avtonomov DM, Mellacheruvu D, Nesvizhskii AI. Msfragger: ultrafast and comprehensive peptide identification in mass spectrometry–based proteomics. Nat Methods **2017**; 14:513–20.
19. Kahn ML, Nakanishi-Matsui M, Shapiro MJ, Ishihara H, Coughlin SR. Protease-activated receptors 1 and 4 mediate activation of human platelets by thrombin. J Clin Invest **1999**; 103:879–87.
20. Somodi L, Debreceni IB, Kis G, et al. Activation mechanism dependent surface exposure of cellular factor XIII

on activated platelets and platelet microparticles. J Thromb Haemost **2022**; 20:1223–35.
21. Alberio L, Safa O, Clemetson KJ, Esmon CT, Dale GL. Surface expression and functional characterization of α-granule factor V in human platelets: effects of ionophore A23187, thrombin, collagen, and convulxin. Blood **2000**; 95:1694–1702.
22. Bubak AN, Como CN, Hassell JE Jr, et al. Targeted RNA sequencing of VZV-infected brain vascular adventitial fibroblasts indicates that amyloid may be involved in VZV vasculopathy. Neurol Neuroimmunol Neuroinflamm **2021**; 9:e1103.
23. Ruberg FL, Berk JL. Transthyretin (TTR) cardiac amyloidosis. Circulation **2012**; 126:1286–300.
24. Nagel MA, Cohrs RJ, Mahalingam R, et al. The varicella zoster virus vasculopathies: clinical, CSF, imaging, and virologic features. Neurology **2008**; 70:853–60.
25. Hottz ED, Azevedo-Quintanilha IG, Palhinha L, et al. Platelet activation and platelet-monocyte aggregate formation trigger tissue factor expression in patients with severe COVID-19. Blood **2020**; 136:1330–41.
26. Jones D, Alvarez E, Selva S, Gilden D, Nagel MA. Proinflammatory cytokines and matrix metalloproteinases in CSF of patients with VZV vasculopathy. Neurol Neuroimmunol Neuroinflamm **2016**; 3:e246.
27. Jones D, Neff CP, Palmer BE, Stenmark K, Nagel MA. Varicella zoster virus-infected cerebrovascular cells produce a proinflammatory environment. Neurol Neuroimmunol Neuroinflamm **2017**; 4:e382.
28. Nagel MA, Choe A, Cohrs RJ, et al. Persistence of varicella zoster virus DNA in saliva after herpes zoster. J Infect Dis **2011**; 204:820–4.
29. Gilden DH, Devlin M, Wellish M, et al. Persistence of varicella-zoster virus DNA in blood mononuclear cells of patients with varicella or zoster. Virus Genes **1989**; 2: 299–305.
30. Gilden DH, Cohrs RJ, Hayward AR, Wellish M, Mahalingam R. Chronic varicella-zoster virus ganglionitis —a possible cause of postherpetic neuralgia. J Neurovirol **2003**; 9:404–7.
31. Mahalingam R, Wellish M, Brucklier J, Gilden DH. Persistence of varicella-zoster virus DNA in elderly patients with postherpetic neuralgia. J Neurovirol **1995**; 1:130–3.
32. Birlea M, Nagel MA, Khmeleva N, et al. Varicella-zoster virus trigeminal ganglioneuritis without rash. Neurology **2014**; 82:90–2.
33. Yang Q, Chang A, Tong X, Merritt R. Herpes zoster vaccine live and risk of stroke among Medicare beneficiaries: a population-based cohort study. Stroke **2021**; 52:1712–21.
34. Imam SF, Lodhi OUH, Fatima Z, Nasim S, Malik WT, Saleem MS. A unique case of acute cerebral venous sinus thrombosis secondary to primary varicella zoster virus infection. Cureus **2017**; 9:e1693.
35. Tu TM, Seet CYH, Koh JS, et al. Acute ischemic stroke during the convalescent phase of asymptomatic COVID-2019 infection in men. JAMA Netw Open **2021**; 4:e217498.
36. Cristian D, Bagatto D. Severe stroke in patients admitted to intensive care unit after COVID-19 infection: pictorial essay of a case series. Brain Hemorrhages **2022**; 3:29–35.
37. Bhavsar A, Lonnet G, Wang C, et al. Increased risk of herpes zoster in adults ≥50 years old diagnosed with COVID-19 in the United States. Open Forum Infect Dis **2022**; 9:ofac118.